

# Additional arguments in favor of true quaternary fission of low excited actinides

D.V. Kamanin<sup>\*,1</sup>, A.A. Alexandrov<sup>1</sup>, I.A. Alexandrova<sup>1</sup>, Z.I. Goryainova<sup>1</sup>,  
E.A. Kuznetsova<sup>1</sup>, A.O. Strelakovsky<sup>1</sup>, O.V. Strelakovsky<sup>1</sup>,  
V.E. Zhuchko<sup>1</sup>, Yu.V. Pyatkov<sup>2</sup>, A.V. Tomas<sup>2</sup>, V. Malaza<sup>3</sup>

<sup>1</sup>Joint Institute for Nuclear Research, Dubna, Russia

<sup>2</sup>National Research Nuclear University "MEPhI", Moscow, Russia

<sup>3</sup>University of Stellenbosch, Saldanha, South Africa

E-mail: kamanin@jinr.ru

DOI: 10.29317/ejpfm.2019030204

Received: 11.05.2019 - after revision

Specific linear structures in the region of a big missing mass in the fission fragments mass correlation distributions were revealed due to effective cleaning of this region from the background linked with scattered fragments. One of the most pronounced structures looks like a rectangle bounded by the magic nuclei. The fission events aggregated in the rectangle show a very low total kinetic energy. We propose possible scenario of forming and decay of the multi-cluster pre-scission configuration decisive for the experimental findings.

**Keywords:** multibody decays, clustering, magic nuclei.

## Introduction

In our experiments dedicated to searching for manifestations of multibody decays of low excited nuclei [1-3] two fragments were actually detected while deficit of their total mass comparing the mass of the mother system ("missing" mass) served a sign of at least ternary decay. The detected fragments fly apart

almost collinearly and at least one of them shows magic nucleon composition. We have called this decay channel “collinear cluster tri-partition (CCT)” in order to underline the likeness with known cluster decay or “lead radioactivity”. One of the most pronounced of the observed decay modes has been already discussed in our previous publications [4, 5]. The revealed features of the process suggest that likely true quaternary fission takes place in this case. The term “true” is used to underline that all the decay products have comparable masses (by analogy with the known term “true ternary fission”). Such kind of the decay of low excited heavy nuclei  $^{252}\text{Cf}$  and  $^{235}\text{U}$  was observed for the first time hence nothing was known about the mechanism of the process. Presented below more profound analysis of the experimental data provides additional arguments in favor of quaternary nature of the decay.

## Experiments and results

The spectrometer used in the experiment was based on the modules of the FO-BOS setup [1]. The TOF-E (time-of-flight vs. energy) method for the measurements of two fission fragments (FFs) masses in coincidence with two detectors placed at 180 degrees was applied. The TOF of the fragment has been measured over a flight path of 50 cm between the “start” detector, placed next to the  $^{252}\text{Cf}$  source and the “stop” detectors formed by position-sensitive avalanche counters (PSAC). PSACs provided also the fragment emission angle with a precision of  $1^\circ$ . The energies of those coincident fragments which passed through the PSACs were measured in the Bragg ionization chambers (BIC). For detecting the isotropic component of the neutrons emitted in fission the “neutron belt” [2] consisting of 140  $^3\text{He}$  filled neutron counters was assembled in a plane perpendicular to the symmetry axis of the spectrometer which serves as the mean fission axis at the same time.

The FFs mass correlation distribution obtained in the experiment is shown in Figure 1a. The events involved were selected applying the selection conditions illustrated by the Figure 1c and Figure 1d.

The rectangular structure marked by the arrow in the center of the graph 1a attracts attention. The low vertex of the structure lies in the vicinity of the point (68, 68) amu associated with magic Ni isotope. The opposite corner of the rectangle presumably corresponds to the  $^{84}\text{Se}$  nucleus (Figure 1b). The yield of the events joined in the structure does not exceed  $10^{-5}$  per binary fission.

Application of the different selection gates allowed to obtain the mass correlation distribution shown in Figure 2a. Only fission events lying inside the box w1 (Figure 2b) and satisfying the condition that at least one neutron was detected ( $n=1$ ) are presented. Specific rectangular structure pointed out in Figure 1a is reproduced but the selection rule used in this case turns out less rigorous and the points inside the rectangle become also selected. A total yield of the filled rectangle has approximately doubled. The total kinetic energy (TKE) of the events in the structure lies in the range (90-140) MeV.

It should be noted that in both cases (Figure 1 and Figure 2) the selection gates were chosen heuristically within criterion of observing any graphic cluster [2, 6].

Special attention was paid to the robustness of the revealed structures against a variation of the selection gates.

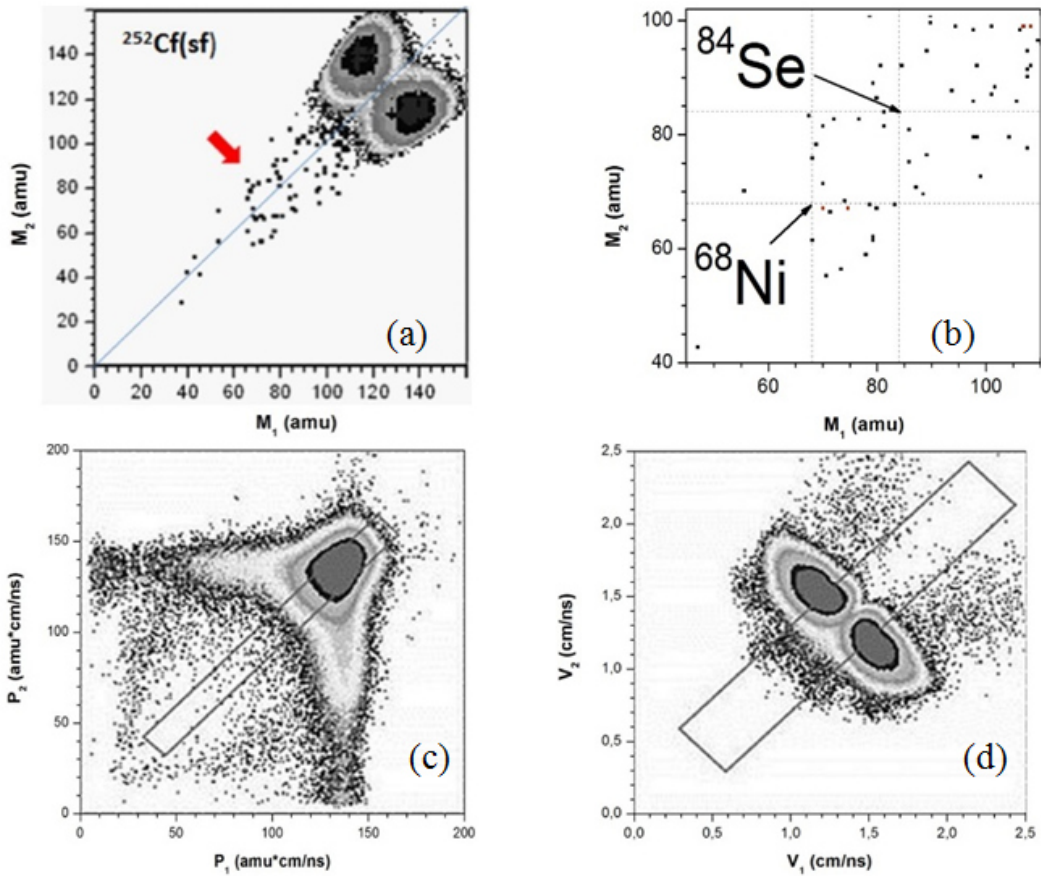


Figure 1. Mass correlation distribution for the FFs from  $^{252}\text{Cf}(\text{sf})$  – (a). The rectangular structure in the center of the graph (marked by the arrow) is under analysis. It is shown in the larger scale in (b). The boxes in (c) and (d) illustrate the selection rule by the momenta and velocities correspondingly. Applying of such selection to the initial FFs mass-mass distribution results in the plot (a).

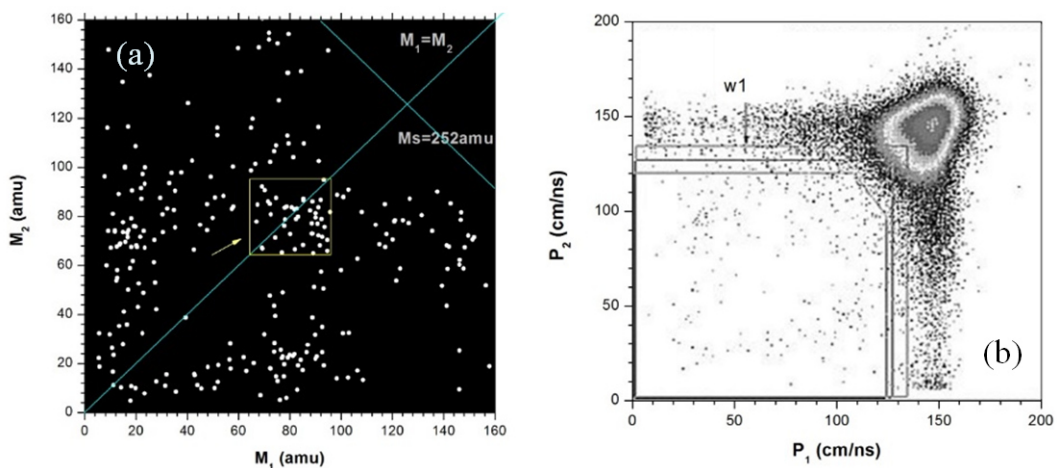


Figure 2. FFs mass correlation distribution from  $^{252}\text{Cf}(\text{sf})$  – (a). The events to be analyzed are marked by the arrow. For all shown points the condition is met that the FFs momenta lie in the box w1 (b) and  $n=1$  (more than one neutron was detected in fission event).

Comparing a total number of events in the plot 2a with similar one for  $n=2$  (does not shown here) in the frame of the mathematical model of the neutron registration channel [2] we came to conclusion that a neutron source which could

provide such difference, corresponds to the multiplicity  $n=2$  if neutrons are emitted isotropically or  $n=7$  if they are emitted from the fully accelerated FFs.

## Kinematic model of the quaternary decay

Analyzing the experimental findings for the events from the box marked by the arrow in Figure 2a we noticed a proximity of the values of the total kinetic energy of two detected fragments  $TKE_2$  and their interaction energy at the Coulomb barrier  $E_b$ . As an example the parameters for the point where two nuclei of  $^{85}\text{As}$  were detected are analyzed below. The nuclear charge of the fragment was calculated according unchanged charge density hypothesis. The parameters known from the experiment and the graph of the nucleus-nucleus potential are presented in Figure 3a.

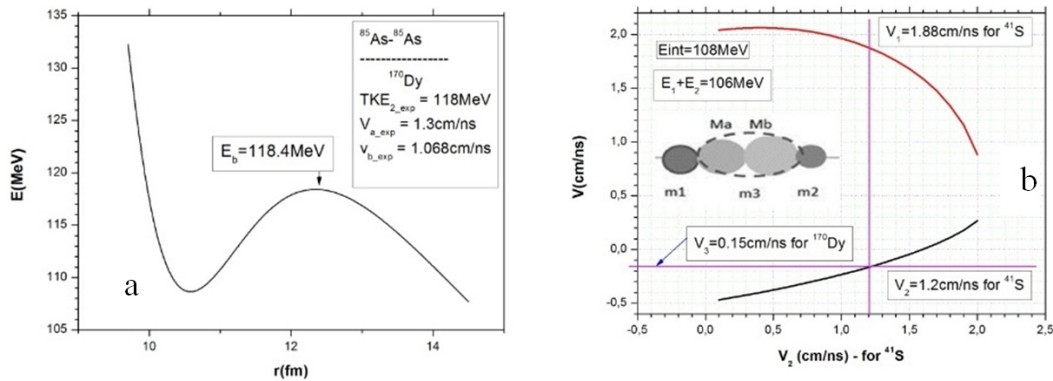


Figure 3. Interaction potential between the nuclei  $^{85}\text{As}$ - $^{85}\text{As}$  – (a). (b) – velocities of the side fragments  $V_1, V_3$  satisfying the system of equations (1) at the interaction energy  $E_{int} = 108$  MeV between the partners of the ternary precission configuration  $^{41}\text{S}$ - $^{170}\text{Dy}$ - $^{41}\text{S}$ . See text for details.

The observing correlation between  $TKE_2$  and  $E_b$  could be if the  $^{170}\text{Dy}$  nucleus being at rest undergoes the break-up onto two  $^{85}\text{As}$  nuclei. In its turn  $^{170}\text{Dy}$  nucleus could stay at rest after simultaneous separation of the side clusters of equal masses in the precission configuration shown in the inset in Figure 3b. Certainly, this is an ideal scenario undergoing deviations in reality.

There is a very simple criterion for testing the proposed scenario. If the central fragment  $m_3$  moves as a whole before the brake-up the velocities of the resultant fragments  $V_a$  and  $V_b$  should meet the conditions:

$$V_a = V^{(a)} + V_0; V_b = V^{(b)} - V_0, \quad (1)$$

where  $V^{(a)}$  and  $V^{(b)}$  are the velocities of the fragments after scission of the central fragment  $m_3$  being at rest. Corresponding energies of these fragments are supposed to be equal to their interaction energy  $E_b$  at the Coulomb barrier:  $E^{(a)} + E^{(b)} = E_b$ .  $V_0$  is the drive velocity of the fragment  $m_3$  before its brake-up. In the case under analysis  $V^{(a)} = V^{(b)} = 1.15$  cm/ns,  $V_0 = 0.15$  cm/ns,  $E_0 \approx 2$  MeV. Results of the similar calculations for all 45 points from the box marked by the arrow in Figure 2a are presented in Figure 4a.

Clear and expected correlation seen in Figure 4a shows that really at the moment of the scission of the central fragment  $m_3$  it flies as a single body with the drive

velocity does not exceed 0.3 cm/ns.

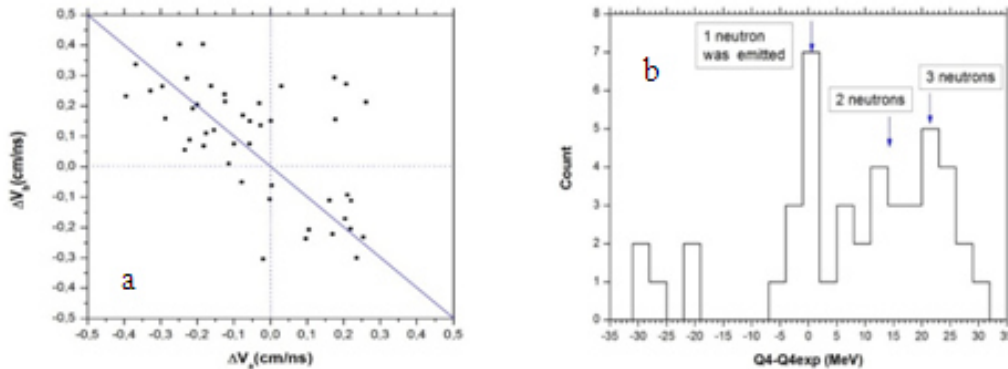


Figure 4. Difference  $\Delta V_a$  between the experimental velocity  $V_a$  of the fragment  $M_a$  (see the inset in Figure 3b) and its expected velocity  $V^{(a)}$  resulting from the binary decay of the central fragment  $m_3$  being at rest. Similar description is valid for the fragment  $M_b$  – (a). Difference between the theoretical and experimental values of the energy release in quaternary decay of  $^{252}\text{Cf(sf)}$  – (b).

Thus, we deal with sequential process. At the first stage a ternary decay takes place whereby two side and the central fragment become free. At the second stage the central fragment undergoes binary brake-up. In order to test energy conservation in the proposed scenario of the quaternary decay we used the following approach.

In case of ternary decay, after full acceleration (at infinity) of all the fragments, both energy and momentum conservation laws should be met:

$$E_1 + E_2 + E_3 = E_{int}, \tag{2}$$

$$\vec{p}_1 + \vec{p}_2 + \vec{p}_3 = 0, \tag{3}$$

where  $E_{int}$  is the interaction energy between the fragments at the beginning of the acceleration;  $E_i$  and  $p_i$  are, respectively, their energies and momenta. Thus, there are three unknown velocities, and one has only two equations for their determination. However, changing step-by-step one of the velocities or energies, we can solve the set of Equation (1) for each fixed value, for instance,  $V_2$  (Figure 3b). According to the algorithm, any vertical line, intersecting both the  $V_2$  axis and the curves above, provides a trio of parameters, namely  $V_1, V_2, V_3$ , satisfying the system (1).

Directly from the experiment only missing mass is known. We suppose it to be the total mass of two side fragments  $m_1, m_2$  equal by masses. The energy releases for different stages of the considered decay are as follows:  $Q_2 (\text{Dy} \rightarrow 2 \text{ }^{85}\text{As}) = 71 \text{ MeV}$ ,  $Q_3 (\text{Cf} \rightarrow \text{}^{41}\text{S}/\text{}^{170}\text{Dy}/\text{}^{41}\text{S}) = 165 \text{ MeV}$ ,  $Q_4 (\text{Cf} \rightarrow \text{}^{41}\text{S}/\text{}^{85}\text{As}/\text{}^{85}\text{As}/\text{}^{41}\text{S}) = 235 \text{ MeV}$ . Expected excitation energy of the  $^{170}\text{Dy}$  nucleus after separation of the side fragments  $E^*(\text{Dy}) = \text{TKE}_{2exp} - E_0(\text{Dy}) - Q_2 + B_n = 55 \text{ MeV}$  under condition that one neutron having binding energy  $B_n$  was emitted. We remind that at least one neutron was detected in coincidence with fission fragments (Figure 2a). Interaction energy of the partners of the ternary decay in the scission point  $E_{int} (\text{}^{41}\text{S}/\text{}^{170}\text{Dy}/\text{}^{41}\text{S}) = Q_3 - E^*(\text{Dy}) = 108 \text{ MeV}$ . All possible velocities of the products of the ternary decay  $\text{Cf} \rightarrow \text{}^{41}\text{S}/\text{}^{170}\text{Dy}/\text{}^{41}\text{S}$  at this value of  $E_{int}$  satisfying the relations

(1) are depicted in Figure 3b. Now it is possible to compare theoretical and experimental energy releases of the quaternary decay  $Q_4 - Q_{4exp} = Q_4 - (\text{TKE}_{4exp}) = (235-232)\text{MeV} = 3 \text{ MeV}$ , where  $\text{TKE}_{4exp}$  is the total kinetic energy of all four partners of the decay. Good agreement can be stated. The spectrum of the difference  $Q_4 - Q_{4exp}$  for all events is shown in Figure 4b. It demonstrates that from one to three neutrons can be emitted (an average of two), what agrees with prediction mentioned above.

## Conclusion

The experimental findings and model analysis indicate that the true quaternary decay of the  $^{252}\text{Cf}(\text{sf})$  goes via very elongated prescission configurations of the mother nucleus. Similar conclusion was drawn in [7] concerning the mechanism of the collinear cluster tri-partition (CCT) of the same nucleus. Presumably the quaternary decay is due to preformation in the valley of the symmetric nuclear shapes of the potential energy surface of  $^{252}\text{Cf}$  specific nuclear shape which looks like a deformed magic core (strong shell minima at  $N \approx 88, 100$  and  $Z \approx 60$ ) and two light clusters on the sides. Further elongation of such system gives rise to the true quaternary decay observed for the first time.

## Acknowledgments

This work was supported, in part, by the Russian Science Foundation and fulfilled in the framework of MEFHI Academic Excellence Project (Contract No. 02.a03.21.0005, 27.08.2013) by the Department of Science and Technology of the Republic of South Africa (RSA), the reported study was funded as well by RFBR according to the research project No 18-32-00538.

## References

- [1] Yu.V. Pyatkov et al., Eur. Phys. J. A **45** (2010) 29.
- [2] Yu.V. Pyatkov et al., Eur. Phys. J. A **48** (2012) 94.
- [3] D.V. Kamanin, Yu.V. Pyatkov, Clusters in Nuclei – Vol. 3 **875** (2013) 183.
- [4] D.V. Kamanin et al., Int. Symposium on Exotic Nuclei EXON-2016, Kazan, (2017) 243.
- [5] Yu.V. Pyatkov et al., Journal of Physics: Conference Series, **863** (2017) 012046.
- [6] Yu.V. Pyatkov et al., NIM A **488** (2002) 381.
- [7] Yu.V. Pyatkov et al., Phys. Rev. C **96** (2017) 064606.